Self-Consistent Interpretation of the 2D Structure of the Liquid $Au_{82}Si_{18}$ Surface: Bending Rigidity and the Debye-Waller Effect

S. Mechler,[1,*] P. S. Pershan,[1] E. Yahel,[1,2] S. E. Stoltz,[1] O. G. Shpyrko,[3] B. Lin,[4] M. Meron,[4] and S. Sellner[1]

[1]*Department of Physics and SEAS, Harvard University, Cambridge, Massachusetts 02138, USA*

[2]*Department of Physics, NRCN, Be'er-Sheva, Israel 84190*

[3]*Department of Physics, University of California San Diego, San Diego, La Jolla, California 92093, USA*

[4]*CARS, University of Chicago, Chicago, Illinois 60637, USA*

(Received 18 June 2010; published 27 October 2010)

The structural and mechanical properties of 2D crystalline surface phases that form at the surface of liquid eutectic $Au_{82}Si_{18}$ are studied using synchrotron x-ray scattering over a large temperature range. In the vicinity of the eutectic temperature the surface consists of a 2D atomic bilayer crystalline phase that transforms into a 2D monolayer crystalline phase during heating. The latter phase eventually melts into a liquidlike surface on further heating. We demonstrate that the short wavelength capillary wave fluctuations are suppressed due to the bending rigidity of 2D crystalline phases. The corresponding reduction in the Debye-Waller factor allows for measured reflectivity to be explained in terms of an electron density profile that is consistent with the 2D surface crystals.

DOI: 10.1103/PhysRevLett.105.186101 PACS numbers: 68.03.Hj, 61.05.cm, 62.25.−g, 68.35.bd

Experiments within the last 15 years have revealed that liquid metallic surfaces generally have a higher degree of order than the corresponding bulk liquid phase. This is manifested in the form of atomic layering normal to the surface that decays within a few atomic distances into the bulk liquid, as was theoretically predicted by D'Evelyn and Rice [1]. Layering was found experimentally in elemental metallic liquids such as, e.g., Ga [2], In [3], Sn, and Bi [4], as well as in liquid alloys such as, e.g., eutectic Bi-Sn [5] and Au-Ge [6]. The atomic arrangement within the topmost layer of most of these liquids is nearly as well defined along the surface normal as those at the surface of crystals. This occurs in spite of the fact that the in-plane atomic order within each surface layer is liquidlike.

The free surface of the liquid phase of the $Au_{82}Si_{18}$ eutectic alloy [7,8] surprisingly shows properties that are dissimilar from all of the other metallic systems that have been studied so far. For temperatures slightly above the bulk eutectic temperature ($T_e = 632$ K) the layering peak observed in x-ray reflectivity at a wave vector transfer normal to the surface $q_z = 2\pi/d$, where d is the interatomic distance, is more than an order of magnitude more intense than for any other metallic liquid. This anomalously high intensity is accompanied by the formation of two dimensional (2D) crystalline surface order [7–10]. At about 12 K above T_e the low-temperature (LT) phase transforms into a high-temperature (HT) phase that consists of different in-plane order. The HT phase remains stable up to at least 50 K above the eutectic temperature. However, the interplay between the anomalous reflectivity and the crystalline surface phases has not been fully understood.

In this Letter we use x-ray scattering measurements to demonstrate that the LT and HT surface phases of liquid $Au_{82}Si_{18}$ consist of atomic bi- and monolayer phases, respectively. Both of these phases exhibit bending rigidity that vanishes when the HT crystals melt into a liquidlike (LL) surface phase. The thermal surface fluctuations of the LL phase do not exhibit any rigidity, in agreement with the basic capillary model [11,12]. The effect of bending rigidity of the LT and HT crystals is to quench the short wavelength surface capillary waves that are responsible for a significant fraction of the Debye-Waller effect that would otherwise reduce the amplitude of the specular reflectivity. By making use of this effect we have been able to develop a picture of the liquid surface structure that is consistent with the constraints imposed by the bilayer interlayer spacing of the LT phase and the rigidity of the LT and HT phases.

Similar examples of surface rigidity induced by thin 2D crystalline systems are Langmuir layers of mono- and bilayer crystals that can form on the liquid water surface [13]. On the other hand, since the thickness of Langmuir monolayers is never less than ~20 Å it is not clear whether they should be treated as 2D systems. From a classical point of view, the long wavelength bending rigidity of extremely thin films should vanish; however, as a consequence of the sp^2 hybridization of the carbon atoms, even monolayer graphene is expected to show finite bending rigidity [14–16]. In fact, this is thought to be crucial for the stability of the monolayer 2D crystals. Measurements of bending rigidity of such thin 2D crystals have only been possible for multilayers with eight or more layers [17].

The experiments were performed at the ChemMatCARS beam line ID-15-C at the Advanced Photon Source, Argonne, IL, USA at x-ray energies of 10 keV for the grazing incidence diffuse scattering data and 11.7 and 11.915 keV for the reflectivity and grazing incidence diffraction (GID) measurements. Rapid parallel

data collection was accomplished through the use of an area detector [18]. Analysis of the liquid surface reflectivity data was performed in a similar way to that described in [2,4,7].

The temperature dependence of the reflectivity of the liquid $Au_{82}Si_{18}$ surface at a fixed specular condition while heating from 625 up to 800 K is shown in Fig. 1(a). In accordance with earlier studies [7] the first abrupt drop in reflectivity at 644 K is identified as a first order transition from the LT to the HT surface phase. The second drop in reflectivity around 705 K is a new, previously unreported result that indicates a first order phase transition of the HT phase into another, laterally disordered surface phase which we refer to as liquidlike (LL) phase. Both phase transitions are reversible.

The discrete Bragg reflections that appear in the GID patterns shown in Fig. 1(b) indicate the presence of long range in-plane crystalline order. Although the relative intensities of the Bragg reflections differ in each measurement, due to the different orientational samplings of the 2D powder distribution, all of the Bragg reflections are observed in every measurement and their positions are identical to those reported previously [7,8]. The absence of discrete Bragg reflections in the corresponding GID pattern LL in Fig. 1(b) demonstrates that the LL phase lacks any crystalline in-plane surface order; i.e., the surface crystals of the HT phase melt into a liquidlike surface layer. The corresponding specular x-ray reflectivity curves for the LT and HT surface phase as well as for the newly discovered LL phase are displayed in Fig. 1(c). The data are normalized to the theoretical Fresnel reflectivity R_F which is the reflectivity of a flat structureless surface with the electron density of the bulk liquid phase. The solid lines are theoretical models that will be discussed below. Although the normalized reflectivity R/R_F of the HT and LL phase is comparable to that observed for other liquid metals and alloys, the amplitude of high-q_z R/R_F data for the LT phase is more than an order of magnitude greater. The origin of this anomalously strong reflectivity of the LT phase is due, in some part, to the bending rigidity of the crystalline surface phase, as is demonstrated below.

Although the reflectivity measurements can be modeled with empirical electron density profiles [7,8] it is now well established that without some sort of constraint such models are not unique [4]. The most meaningful new constraints reported here are the thicknesses of the 2D crystals of the LT and HT phases obtained from the truncation rod data shown in Fig. 2. Figures 2(a) and 2(b) show the intensity distribution in the q_{xy}-q_z plane of selected Bragg reflections of the crystalline surface phases of the LT phase ($q_{xy} \approx 1.833$ Å^{-1}) and of the HT phase ($q_{xy} \approx 2.665$ Å^{-1}). The most relevant new result is the intensity minimum at $q_z \approx 0.95$ Å^{-1} for the LT phase that can be contrasted with the smooth monotonic decay for the HT truncation rod. Note also that the truncation rods are virtually parallel to the surface-normal q_z axis indicating

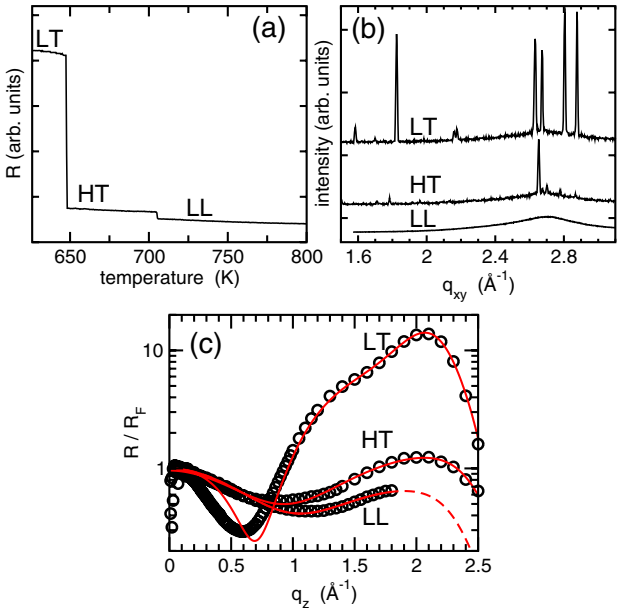

FIG. 1 (color online). (a) Temperature dependence of x-ray reflectivity from liquid $Au_{82}Si_{18}$ at a wave-vector transfer q_z of 1.4 Å^{-1} during heating at a rate of 5 K/min. The three different temperature regimes that are visible define three surface configurations: low-temperature (LT), high-temperature (HT), and liquidlike (LL). (b) Grazing incidence diffraction patterns of the three surface phases at 635 K for LT phase, 695 K for HT, and 720 K for LL. (c) Fresnel-normalized reflectivity R/R_F for LT, HT, and LL phases. The solid lines represent the best fit to the data using the electron densities shown in Fig. 3(c). The dashed line illustrates the extension of fitted R/R_F of the LL phase to higher values of q_z.

that both crystalline phases are 2D lattices. Figure 2(c) shows intensities obtained by integration of truncation rods for the LT and the HT surface crystals over the q_{xy} direction. For the LT phase the two truncation rods of Bragg reflections at $q_{xy} \approx 1.833$ Å^{-1} and $q_{xy} \approx 2.633$ Å^{-1} show intensity minima at $q_z \approx 0.95$ Å^{-1} that correspond to destructive interference at a length scale $d_{\mathrm{bi}} = \pi/q_{\mathrm{min}} \approx 3.31$ Å. The existence of the minimum at this length scale, i.e., the vanishing of the intensity of the Bragg reflection, was observed for all the observable Bragg reflections shown in Fig. 1(b) [18]. The combination of the GID and truncation rod data clearly indicates that the LT phase contains a bilayer composed of two 2D crystalline atomic layers directly above one another. In contrast, the monotonic decay of the truncation rod intensity for the Bragg reflection of the HT phase at $q_{xy} \approx 2.665$ Å^{-1} indicates that this phase consists of 2D crystalline monolayers.

As was previously demonstrated for Langmuir layers on water [13,19], bending rigidity of the surface phases can be directly obtained from measurement of grazing incidence diffuse scattering arising from the height-height correlations associated with thermal capillary waves. Such data for the LT and the LL phases of the liquid Au-Si eutectic

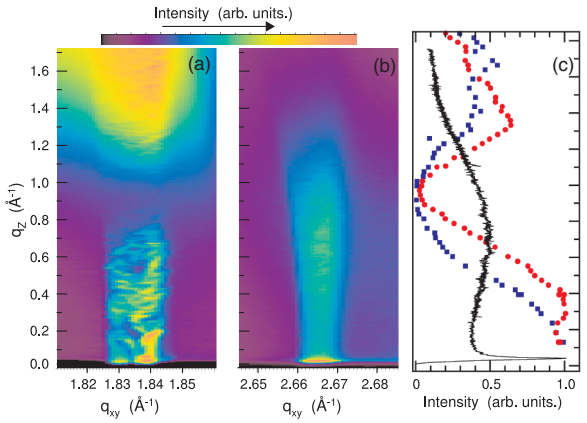

FIG. 2 (color online). (a),(b) Crystalline truncation rods of selected Bragg reflections collected with the area detector for the LT phase (a) and the HT phase (b). The inhomogeneous distribution of intensities for the LT truncation rod is due to the finite grain size of the relatively coarse 2D surface crystals. (c) Integrated intensities of truncation rods for Bragg reflections of the LT crystals [$q_{xy} = 1.833$ Å^{-1} (circles) and $q_{xy} = 2.633$ Å^{-1} (squares)] and of the HT crystals [$q_{xy} = 2.665$ Å^{-1} (black line)] [18]. The data are normalized to the highest intensity within the respective truncation rods.

are shown in Fig. 3(a). The data for the LL phase agree perfectly with the $1/\gamma q_{xy}^2$ power law that is expected for capillary wave fluctuations governed by surface tension γ without any bending rigidity term.

On the other hand, explanation of the data for the LT phase requires bending rigidity κ that we associate with the surface crystals. This is demonstrated by the solid line through the data that corresponds to scattering cross-section term scaling as $(\gamma q_{xy}^2 + \kappa q_{xy}^4)^{-1} = \gamma^{-1} q_{xy}^{-2}(1 + q_{xy}^2/q_e^2)^{-1}$ with the elasticity cutoff wave vector $q_e = \sqrt{\gamma/\kappa} = 0.08$ Å^{-1} [20,21]. For q_{xy} less than about 0.02 Å^{-1} the slope for the LT and LL phases is indistinguishable. It is worth noting that the bending rigidity κ of the surface crystals does not influence the thermal excitation spectrum for long wavelength capillary waves. This is shown by comparison of the long wavelength diffuse scattering data for the LT, HT, and LL phase that are shown in Fig. 3(b). For these data, with $|q_{xy}| \leq 0.02$ Å^{-1}, the detector angle β deviates only slightly from the specular condition at the incident angle. On the other hand, as we will discuss below the only way to simultaneously account for the amplitude of both the diffuse scattering and R/R_F for the HT phase [18], as well as the shape of the diffuse scattering is to include rigidity.

The reflectivity R/R_F of a liquid surface can generally be described by [8]:

$$R(q_z)/R_F(q_z) = \mathrm{CW}(q_z)|\Phi(q_z)|^2, \qquad (1)$$

where $|\Phi(q_z)|^2$ denotes the surface structure factor normal to the surface and the effective Debye-Waller factor of thermal capillary waves, $\mathrm{CW}(q_z)$, is given by integration of

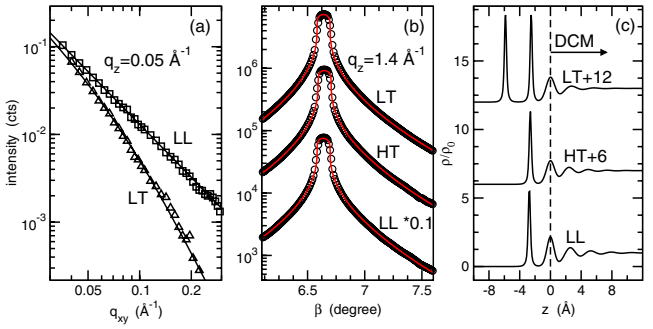

FIG. 3 (color online). (a) Grazing incidence diffuse scattering data of the $Au_{82}Si_{18}$ liquid for the LT and LL surface phases at $q_z = 0.05$ Å^{-1}. The solid lines represent fits to the $1/\gamma q_{xy}^2$ power law for the LL phase and the $(\gamma q_{xy}^2 + \kappa q_{xy}^4)^{-1}$ form that includes bending rigidity κ of the LT phase. (b) Off-specular diffuse scattering of the $Au_{82}Si_{18}$ liquid at a small angle β away from the specular condition ($\alpha \equiv \beta = 6.64°$ and $q_z = 1.4$ Å^{-1}) for the surface phases LT, HT, and LL. The data are broadened along q_z using an electronic slit on the area detector to circumvent complications associated with the singularity at $\alpha = \beta$ [18]. The solid lines are fits using the theoretical scattering cross section of the capillary wave model [3] including the elasticity cutoff wave vector q_e. (c) Electron density profiles normal to the surface for the LT, HT, and LL phases that were obtained by recursively fitting the reflectivity R/R_F [see Fig. 1(c)] and the off-specular diffuse scattering [see Fig. 3(b)]. Data in (b) and (c) are offset vertically as indicated for clarity.

$$\mathrm{CW}(q_z) = \int_{A_{q_{xy}}} d^2 q_{xy} \left(\frac{q_{xy}}{q_{\max}}\right)^{\eta} \frac{\eta}{2\pi q_{xy}^2} \qquad (2)$$

over the reciprocal space area defined by the experimental resolution. The capillary exponent is $\eta = (k_B T/2\pi\gamma)q_z^2$.

For the LL phase, as well as for the surfaces of all of the liquid metals that have been studied thus far, $q_{\max}$ is the cutoff (Debye) wave vector of capillary waves of the system. For a liquidlike surface $q_{\max}$ usually is taken to be determined by the atomic diameter d_{at} [22], i.e., $q_{\max} = \pi/d_{\mathrm{at}} = 1.16$ Å^{-1} with $d_{\mathrm{at}} = 2.70$ Å for Au. Taking into account the bending rigidity for the surface crystals in the LT and HT phases it can be shown that within the region of interest of $q_{\max} \gg q_e \gg 1/\xi_{\mathrm{corr}}$, with the x-ray coherence length $\xi_{\mathrm{corr}} \geq 1$ μm, the contribution of capillary waves is similar to Eq. (2) except that $q_{\max}$ is replaced by the elasticity cutoff wave vector q_e. The effect of $q_e \ll q_{\max}$ is to increase $\mathrm{CW}(q_z)$ [Eq. (2)] such that the measured value of R/R_F could now be fit with a value of $|\Phi(q_z)|^2$ that is smaller than would otherwise be possible. This is fortunate since the smaller value is dictated by the constraints of the bilayer-monolayer structures that are imposed by the GID measurements. For example, according to these measurements the electron density surface profile for the LT phase must be constructed with only two prominent peaks separated by $d_{\mathrm{bi}} = 3.31$ Å that characterize the crystalline bilayer. The underlying liquid is described by further lower-amplitude layers with the same distorted crystal model [23] that is commonly used to describe the surface layering for other liquid metals [see Fig. 3(c)]. For

the HT phase the two prominent peaks are replaced by only a single prominent peak that describes the crystalline monolayer. For the LL phase the electron density profile was obtained by the best fits to the data using the profile for the HT phase as the starting model.

In fact, the only way in which it is possible to self-consistently fit both the reflectivity and off-specular diffuse scattering for the LT and HT phases (the solid lines in Figs. 1(c) and 3(b), respectively) with such a model is by introducing bending rigidity of the 2D surface crystals, treating q_e as a free parameter. For the LT phase we obtain the value of $q_e = 0.10$ Å^{-1}, in good agreement with the value measured directly using GID diffuse scattering in Fig. 3(a). For the HT phase $q_e = 0.40$ Å^{-1}. The corresponding profiles for the electron density normal to the surface for the HT, LT, and LL phases are shown in Fig. 3(c) [18]. Were it not for the observation of the GID peaks it would have been very difficult to distinguish between the HT and LL phases. As can be seen from their reflectivities in Fig. 1(c) and the corresponding profiles in Fig. 3(b) the structure along the surface normal for these two phases is nearly identical. On the other hand, with the knowledge of the 2D order in the HT phase these slight differences are readily accounted for by the difference between q_e and $q_{\max}$. For example, for a wave-vector transfer q_z of 1.8 Å^{-1} the effect of $q_e \approx 0.4$ Å^{-1} for the HT phase is to decrease the contribution of capillary waves to the reflectivity R/R_F by a factor of $\sim$2 and by $\sim$5 for LT with $q_e \approx 0.1$ Å^{-1} [18].

The discovery of the surface stiffness effect thereby yields a physically more plausible and self-consistent picture of the surface structure than previously reported in [7,8] which did not take into account the surface stiffness effect of the 2D crystals. Instead, in order to increase the amplitude of $|\Phi(q_z)|^2$ the electron density profile was constructed using 5–6 sharp peaks that are not consistent with the GID measurements. Furthermore, it is now clear that the intriguing observation in [7] that the surface of the LT phase appeared to show a liquidlike capillary wave behavior is due to the small q_{xy}- range covered by these measurements.

The measured values for the q_e of the LT and HT surface phases correspond to values of the bending rigidity $\kappa \approx 150$ kT for the LT phase and $\kappa \approx 6$ kT for the HT phase. As one would expect the bending rigidity for the bilayer is substantially larger than for the monolayer. Note that the values theoretically predicted for monolayer graphene of $\kappa \approx 50$ kT [14,16] are in between that of the LT and HT phases. The bending rigidity of graphene is thought to arise from multibody atomistic interactions like the bond angle distribution [14,15]. Given the relatively strong C-C directional bonding compared to the weak Au bonding, rigidity of monolayer graphene should be expected to be substantially larger than that of the surfaces phases of liquid eutectic Au-Si.

In summary, we have demonstrated that the surface of liquid $Au_{82}Si_{18}$ undergoes a crystalline 2D bilayer to 2D monolayer transition. The monolayer crystals melt at about 60 K above the eutectic temperature. By means of complementary methods values of bending rigidity of crystalline 2D bi- and monolayer phases are obtained. The surface bending rigidity reduces the amplitude of the contribution of thermally excited capillary waves to the specular reflectivity, resulting in a self-consistent picture of the surface structure of liquid $Au_{82}Si_{18}$.

Research supported by the U.S. Department of Energy, Office of Basic Energy Sciences, Division of Materials Sciences and Engineering under DE-FG02-88ER45379. ChemMatCARS is principally supported by the National Science Foundation/Department of Energy under Grant No. NSF/CHE-0822838. The Advanced Photon Source is supported by the U.S. Department of Energy, Basic Energy Sciences, Office of Science, under Contract No. W-31-109-Eng-38. S. M. is supported by the German Research Foundation through Grant No. Me 3113/2-2. O. S. acknowledges support from NSF CAREER Grant No. 0956131. Help of C. Leistner from HZB, Berlin, Germany in preparing the alloy is greatly appreciated.

*smechler@seas.harvard.edu

[1] M. P. D'Evelyn and S. A. Rice, Phys. Rev. Lett. **47**, 1844 (1981).
[2] M. J. Regan *et al.*, Phys. Rev. Lett. **75**, 2498 (1995).
[3] H. Tostmann *et al.*, Phys. Rev. B **59**, 783 (1999).
[4] P. S. Pershan *et al.*, Phys. Rev. B **79**, 115417 (2009).
[5] O. G. Shpyrko *et al.*, Phys. Rev. Lett. **95**, 106103 (2005).
[6] P. S. Pershan *et al.*, Phys. Rev. B **80**, 125414 (2009).
[7] O. G. Shpyrko *et al.*, Science **313**, 77 (2006).
[8] O. G. Shpyrko *et al.*, Phys. Rev. B **76**, 245436 (2007).
[9] A. L. Pinardi, S. J. Leake, R. Felici, and I. K. Robinson, Phys. Rev. B **79**, 045416 (2009).
[10] T. U. Schuelli *et al.*, Nature (London) **464**, 1174 (2010).
[11] S. K. Sinha, E. B. Sirota, S. Garoff, and H. B. Stanley, Phys. Rev. B **38**, 2297 (1988).
[12] F. P. Buff, R. A. Lovett, and F. H. Stillinger, Phys. Rev. Lett. **15**, 621 (1965).
[13] J. Daillant *et al.*, Soft Matter **5**, 203 (2009).
[14] Q. Lu, M. Arroyo, and R. Huang, J. Phys. D **42**, 102002 (2009).
[15] M. Arroyo and T. Belytschko, Phys. Rev. B **69**, 115415 (2004).
[16] E. Cadelano, S. Giordano, and L. Colombo, Phys. Rev. B **81**, 144105 (2010).
[17] M. Poot and H. S. J. van der Zant, Appl. Phys. Lett. **92**, 063111 (2008).
[18] See supplementary material at http://link.aps.org/supplemental/10.1103/PhysRevLett.105.186101 for further information.
[19] C. Gourier *et al.*, Phys. Rev. Lett. **78**, 3157 (1997).
[20] J. Meunier, J. Phys. (Paris) **48**, 1819 (1987).
[21] H. Kellay and J. Meunier, J. Phys. Condens. Matter **8**, A49 (1996).
[22] O. Shpyrko *et al.*, Phys. Rev. B **67**, 115405 (2003).
[23] O. M. Magnussen *et al.*, Phys. Rev. Lett. **74**, 4444 (1995).